

Engineered Science

DOI: https://dx.doi.org/10.30919/es1557



Nitrate-base Molten Salts Platform as Thermal Energy Storage in Thermocline Tank for Thermal Solar Pyrolysis Unit

Nattadon Pannucharoenwong,^{1,2} Snunkhaem Echaroj,^{1,2,*} Suwipong Hemathulin,^{2,3,*} Direk Nualsing,^{1,2} Rangsan Wannapop^{1,2} and Phadungsak Rattanadecho¹

Abstract

This research aimed to establish a thermal solar pyrolysis unit powered by molten salt flow from thermocline tank. Encapsulated graphene oxide in silica oxide (SiO₂) was employed as a heat transfer agent to facilitate proper heat transfer inside the thermocline tank. Characterization was performed by scanning electron microscope (SEM), differential scanning calorimeter (DSC) and X-ray diffractometer (XRD) techniques to analyze textural morphology and heat storage capacity of the molten salt system. Encapsulation was found to be successful in providing stable matrix to house molten salt and graphene oxide nanoparticles. Addition of graphene oxide in the encapsulated molten salt was found to reduced melting temperature and crystallization temperature by almost 10%, which is help reduce energy required to activate the flow of molten salt inside the thermal system. Charge and discharge cycle were performed by varying molten salt flowrate into thermocline tank. Temperature monitored in axial direction revealed an increase in heat transfer efficiency as flowrate increased. Pyrolysis reaction was also tested using three different catalysts including zeolite, dolomite and kaolin to produce biooil, biochar and gas. An increase in temperature was found to favor gas production over zeolite catalyst due to presence of acidic sites. Optimized pyrolysis to produce 61.0% biooil was performed at 300 °C over kaolin catalysts.

Keywords: Pyrolysis; Molten salts; Thermocline tank; Heterogeneous catalyst. Received: 17 March 2025; Revised: 20 May 2025; Accepted: 25 May 2025.

Article type: Research article.

1. Introduction

Due to inadequate fossil-based energy and high carbon emissions, it is increasingly important to seek other sources of renewable energy. According to a climate change report from Kyoto protocol committee, carbon emissions from electricity generation sector accounted for 25 to 30% of the total emissions. [1] As demand for electricity increases, the higher energy input requirement led governments worldwide to

Email: snunkha@engr.tu.ac.th (S. Echaroj); suwipong@snru.ac.th (S. Hemathulin)

employ various decarbonization technologies to help liberate the electricity sector from its dependence on fossil-based energy. For this reason, the share of renewable energy in 2040 was forecasted at 60% of the total electricity production.^[2] In order to achieve this target, a few obstacles need to be overcome including the cost of technology and uncertainty of energy sources. Energy from waste plastic is an effective source of energy, because it also solve waste disposal problems along with the persisting energy crisis. A pyrolysis process can convert waste plastic to bio-oil usable as transportation or heating fuel. However, the main disadvantage of a pyrolysis process is that it requires intensive input of electricity which may offset its benefit as a source of clean energy. A solar-based pyrolysis unit can be a solution to this problem. For this solar-base technology to perform well, it is important for the system to be assisted by a high efficiency storage system. A thermal solar pyrolysis will be dependent on the efficiency of the thermal energy storage (TES) system. The main role of a TES system in a thermal solar pyrolysis is to storage excess energy harnessed during the day so that electricity can also be generated at nighttime when demand can usually peak in some communities. The main important

¹ Department of Mechanical Engineering, Faculty of Engineering, Thammasat School of Engineering, Thammasat University, Pathum Thani, 12120, Thailand

² Research Unit of Energy Innovation for the Automotive Industry (EIAI), Department of Mechanical Engineering, Faculty of Engineering, Thammasat School of Engineering, Thammasat University, Pathum Thani, 12120, Thailand

³ Department of Mechanical and Industrial, Faculty of Industrial Technology, Sakon Nakhon Rajabhat University, Sakon Nakhon, 47000, Thailand

Research article Engineered Science

characteristic of the TES system is the type of molten salts used, and the design of tank used to circulate molten salts in liquid form.

Molten salts are frequently employed in a TES system because of their high heat capacity, stability property in a wide operating temperature and availability in the market. Unlike phase change materials (PCM) that relied mainly on the release of latent heat as phase changes, molten salt relied on sensible heat inside the tank. However, current complex of molten salts such as solar salt (60% NaNO₃: 40% KNO₃), hitec salt (7% NaNO₃, KNO₃:NaNO₂ and sodium chloride (NaCl) have melting temperature of 580 °C, 538 °C, and 845 °C.[3] A higher phase change temperature indicated that the transformation of solid salts to liquid form required a larger magnitude of energy input. In addition to melting temperature, corrosive rate is also an important consideration factors in decision making. Some salts such as NaCl have a corrosive rate on stainless-steel (SS304 and SS316) as high as 7.2 mm per year.[4,5] Due to these undesirable characteristics of molten salt, a novel technology was developed to encapsulate metal oxide in molten salts complex. [6] Macro porous matrix of threedimensional expanded vermiculite have been employed to attain a 90% energy storage efficiency and provided 613 J/g of energy density when encapsulated with nitrate base salt.[7] Paraffins blocks were used to tune pore size of aluminum oxide so it can encapsulate eutectic chloride salt, which demonstrated a energy storage densities of 272.58 J/g.[8] In addition to the usage of different types of molten salts, it is also important to find an optimal design of the storage tank. Conventionally, a thermal energy storage would consist of two tanks: one for cold molten salt and another one for hot molten salt. These two streams flow back and forth depending on the status of energy usage (charging mode or discharging mode). A two-tank system uses large amount of electricity and also expensive because two set of equipment are needed to be purchased. Recent development of a thermocline tank for thermal storage has been promoted to overcome these problems.

A thermocline system consists of both cold and hot layers of molten salt in one single tank. Alternation between charge and discharge mode is possible by changing the flow direction of molten salt. One of the main characteristics of a thermocline tank is the diffusion system at the inlet of the tank. The diffusion system contained small nozzle which convert laminar flow molten salt into smaller droplet, which help intensify mixing inside the tank and ultimately reduce thermocline layer during both charging and discharging activities.[9] Movement of the thermocline layer whether upward or downward depended on the process of energy replenishment, temperature gradient and imbalance load demand. For this reason, hot section inside the tank behaves like a spring which can shirk and expand depending the interaction between heat transfer medium in the system.[10] Solid fillers such as alumina, quartz and polymer have also been found to enhance the natural stratification inside the

tank.^[11,12] This is due to the buoyancy effects when solid material is immersed in molten salt solution.^[13,14] In case a spheroidal filler materials, the percentage vacancy of the fixbed is from 0.3 to 0.4.^[15] Flow uniformity can be improved by reducing filler size and avoiding fluidization, but at the expense of higher pressure. Problem regarding flow of molten salt along tank wall can be minimized by keeping the talk-to-particle diameter ratio between 30 to 40.^[16] Currently, thermocline tank has been applied as part of thermal energy storage in a district heating system and concentrated thermal solar powerplant.^[17] Additionally, a novel cone guidance system was proposed by Canli at el. to increase mixing intensity as molten salt flow inside the tank.^[18] Combined with a shell-tube heat exchanger with efficient configuration, the electricity generation system can be fully optimized.

Pyrolysis is a chemical process that relied on heat and acid catalyst to breakdown structure of hydrocarbon molecules. Application of pyrolysis varies greatly depending on the input feedstock which have included cellulosic materials, [19,20] algae, vegetable oil,[21] waste oil and plastic waste.[22] Pyrolysis of plastic waste into bio-oil have been regarded one of the major applications of technology and obligated in many countries due to waste reduction mandate and regulation constrains. Different types of plastics can be used for the pyrolysis reaction including polyethylene, higher density polyethylene and low-density polyethylene. Combination of polypropylene with other types of plastic was found to have a positive impact on the pyrolysis reaction. In addition to PE waste, polyethylene terephthalate (PET) can undergo the pyrolysis reaction to produce either monoethylene glycol or terephthalic acid at temperature between 400 °C to 600 °C. Thermal degradation of HDPE was found to begin between pyrolysis temperature 364 to 400 °C. Further increase in pyrolysis temperature to approximately 520 °C can cause pyrolysis reaction to be completed.[23] Other plastic wastes such as Polyvinyl chloride (PVC) and polystyrene. However, calorimeter analysis revealed bio-oil from HPDE and LPDE have the highest heating value of approximately 40 to 48 MJ/kg and viscosity in the range of 1.4 to 1.6 CSt.[24-26]

Co-pyrolysis of PET with biomass such as Samanea saman at ratio of 3:1 (plastic:biomass) demonstrated lower activation energy.[27] Most successful pyrolysis process relied on usage of acidic heterogenous zeolite catalyst, kaolite, and dolomite solid. In addition to active site for pyrolysis reaction and control biochar formation, these catalysts also contain large pore diameters which offer high accessibility and stability for reaction at high temperature. [28,29] These type of catalysts also have a variety of particles with bulk density which help facility heat transfer in the reaction zone. Spent catalyst from catalytic cracking process (combination of zeolite, binder and filler) was employed at a catalyst-to-plastic ratio of 0.2 at pyrolysis temperature of 350°C to yield approximately 78% bio-oil liquid.[26] An increase in undesirable aromatic content in biooil was observed as the amount of catalyst used during pyrolysis increases. It is also pointed out that the increase in

aromatic does not have major impact on the characteristic biooil when used as transportation fuel. One of the main challenges in pyrolysis of plastic is the heat transfer capability inside the reactor which if conducted in a batch-like process may contain dead zone where heat does not reach. Therefore, reactors needed to be assisted with a reliable and continuous flow of heat throughout the reaction zone in absence of oxygen.[30,31]

Till now, various combination of molten salts has been investigated inside a thermocline tank, while the performance encapsulated molten salt in a thermocline tank is rarely documented. Graphene oxide (GO) was used as a carrier while molten salts is encapsulated in a thin layer of silica oxide (SiO₂). GO was chosen because it can help improve thermal conductivity of the encapsulated material. Additionally, GO contained large quantity of oxygen functional sites where SiO₂ capsule can be attached to. This research aimed to investigate the charging and discharging effectiveness of the encapsulated molten salt system inside thermocline tank with a temperature range of 300 to 50 °C. A response surface from polynomial equation derived from experimental data was created to optimize significant parameters including the percentage by weight of graphene oxide used to support encapsulated molten salts, filer particle sizes, and molten salt flow rate. Bioactive encapsulations were also developed to delay medicine dissociation in blood stream using organic substrate. Additionally, other encapsulation catalysts were fabricated in biochar matrix such as cobalt precious metals[32] and zeolite matrix,[33] which construct both hollow structure and yolk-like structure. After establishing an optimum setup for energy storage in molten salt, the heating system was used to pyrolyzed plastic waste in a tubular reactor with spiral coil heating section and heterogenous catalysts (Zeolite). Output derived from both systems includes mainly bio-oil which can be treated and used for transformation fuel and biochar. A sustainable solar based system can be established using solar array with concaved channels as heat source. However, in order to control the system charging of the thermal storage system was conducted with an electric heat source.

2. Experimental

2.1 Fabrication of encapsulated nitrate-base molten salts on graphene oxide platform.

The encapsulation of nitrate-base molten salts (solar salt) can be conducted in three main steps. A measured amount of GO was added to cyclopentyl methyl ether (CPME) solution (20 mL) and stirred for 20 minutes at 30 °C under agitation speed of 600 rpm. Molten salts were obtained by dissolving 10 g of solar salts in 30 mL of DI water in a 200 mL flask. The GO in CPME solution was combined with non-ionic surfactant (Polysorbate 20), poured into the flask with molten salts mixture and agitated 3 hours. GO in CMPE and the non-ionic surfactant will form a bulk hydrophobic layer with open-end hydrophilic tails. These hydrophilic tails can then be attached to molten salts in the solution which will then be the structure

for the inner core of the encapsulation. Consequently, 15 mL of tetraethyl orthosilicate (TEOS) as source of silica oxide (SiO₂) was slowly added to the molten salt solution and agitated continuously for 2 hours. Since TEOS is an amphiphilic molecule, it will be attached to the hydrophobic section (consisting of GO and non-ionic surfactant), which then encapsulates molten salt solutions. Next, hydrolysis of TEOS was conducted afterward via sol-gel reaction to form silicon hydroxide. Hydrolysis was performed by adding NH₄OH dropwise into the combined solution while under constant agitation. Afterward, the sol-gel solution was centrifuged, solid separated, and dried in a open at 120 °C for 10 hours. Solid material collected afterward is the encapsulated molten salt in graphene oxide platform (SiO₂-Encap.salt/GO).

2.2 Operating thermocline tank as thermal energy storage system

This research consists of two different phases including developing thermal source of energy and pyrolysis reaction as shown in Fig. 1. Solar concentrators in the shape of parabolic channel were employed to collect thermal energy during the day. It is connected to the pyrolysis reactor by stainless steel pipe, check valves and pressure regulator. The first phase corresponded to investigation of a thermal energy storage system using encapsulated molten salt. Once the system was successfully developed to improve heating capacity, a thermocline tank with encapsulated molten salt was use to heat reactor for the pyrolysis of waste plastic bag. The thermal energy storage operation was conducted in a 1.5 meter thermocline tank (0.4 meter diameter) with a volume of 0.19 m³. An electric heater (50 LW) was used as a heat source to investigate the charging process. The storage capacity calculated in the temperature range of 300 °C to 500 °C was approximately 65 kWh. Nitrate-based molten salt used was heat transfer fluid in the thermal energy storage system consisted of NaNO₃ (50%), KNO₃ (30%), and LiNO₃ (20%). One of the main characteristics of a thermocline tank is the inlet diffuser designed to distribute and reduce the system of molten salt droplet as it enters the tank. Thermocouples are inserted into the center and the surface of the tank to monitor temperature gradient along different parts of the tank. The thermocouples are placed at an interval of 10 cm from top to bottom of the tank (thermocouples in the range of 200 to 600 $^{\circ}$ C and error of ± 1 K).

Two high temperature resistant pumps are used to initiate charging and discharging separately. A two-tank system was used as thermal storage system as shown in Fig. 2. The first tank (same dimension as thermocline tank) was used to turn molten salt into liquid form so it can be circulated throughout the system. While the system charges, the first pump and ball valve were open to deliver liquid molten salt from first tank to the electric heater and then into the thermocline tank. Heat was transferred from the thermally charged molten salt to spherical fillers, which help absorb and storage thermal heat. Molten salt

Research article **Engineered Science**

discharge phase, the flow direction is reversed with the third pump which delivered hot molten salts from the thermocline tank to the heat exchanger, which represents heat sink or usage of thermal heat. After heat transfer from molten salt inside the heat exchanger, the cooler molten salt was delivered back to the thermocline tank to accumulate and push hotter molten salt out of the tank again. Circulation of molten salts during 2.3 Effectiveness analysis discharge phase was also made possible by the second pump. In order to compare different operational parameters three

circulation is accomplished by the second pump. During The flow rate of the circulation both during charge and discharge phase can be adjusted from the two pumps. Every part of the system is under insulation to avoid thermal loss while the process operates. Each experimental trial was conducted three times to obtain statistical data such as mean, standard deviation and standard error.

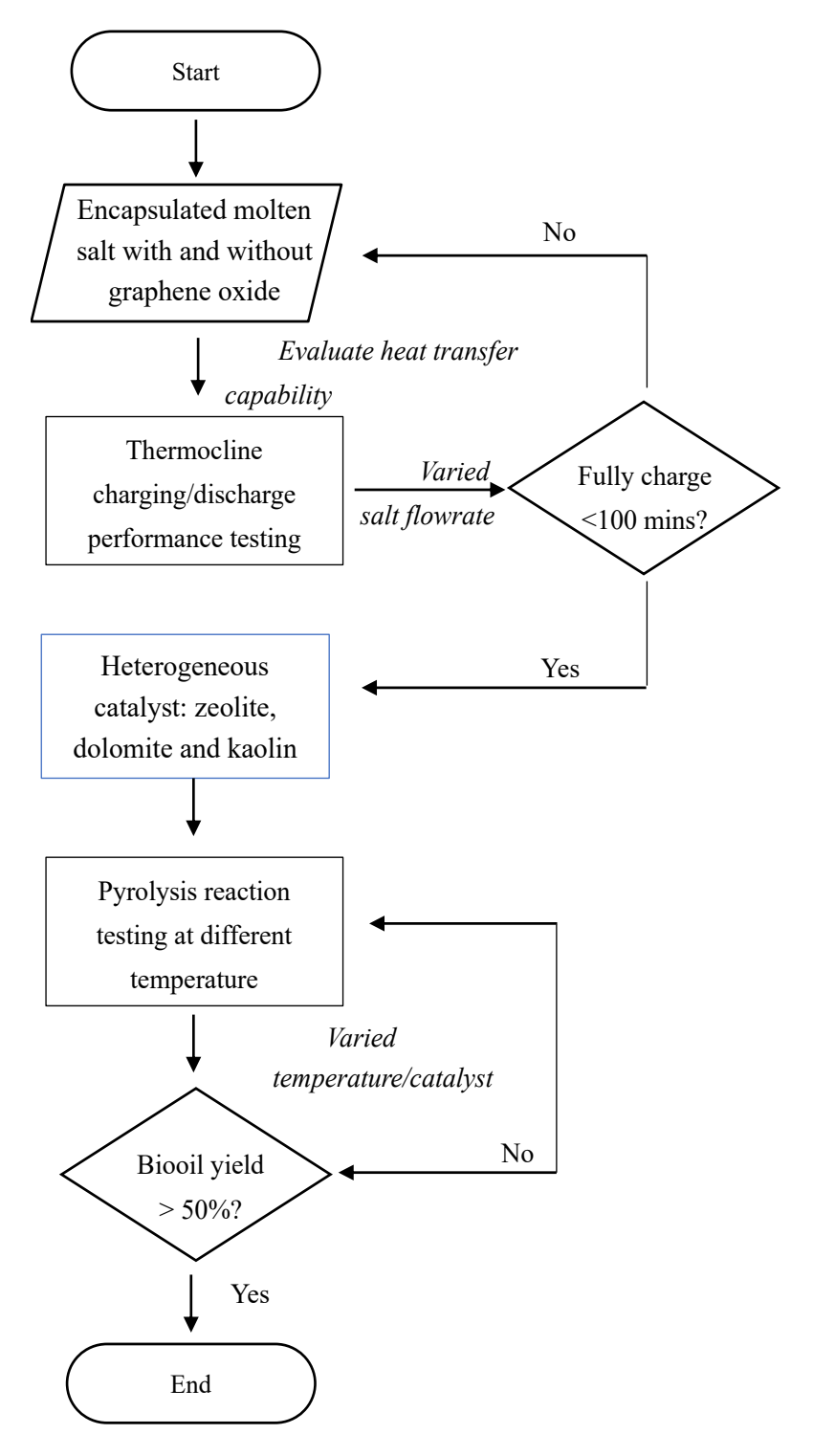


Fig. 1: Flowchart diagram consisting of thermal performance testing and pyrolysis testing over different temperatures and catalysts.

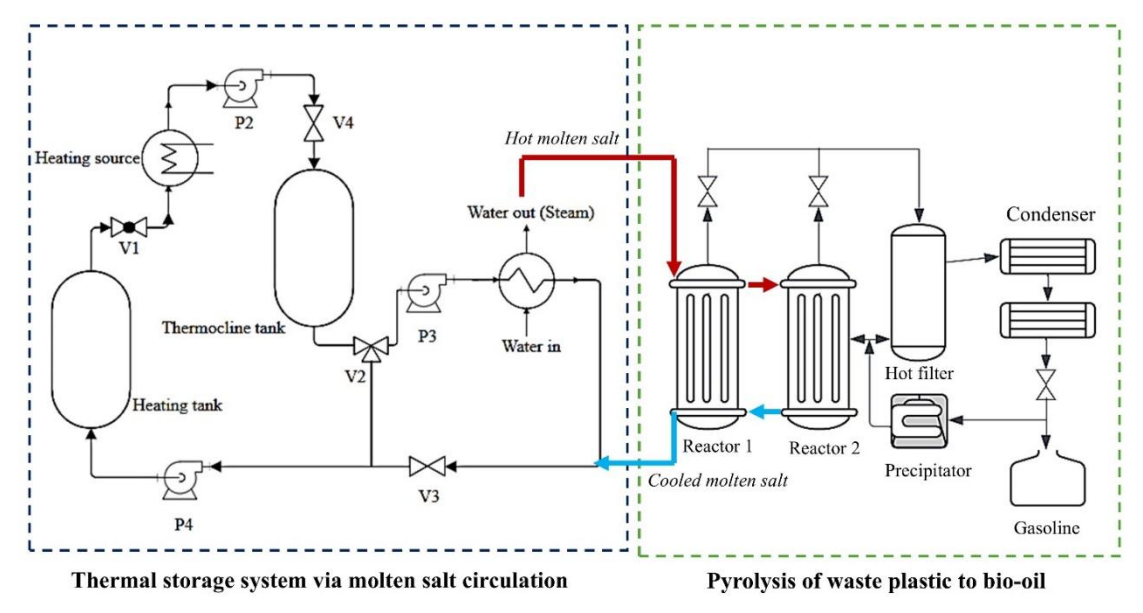


Fig. 2: Systematic diagram of discharge/charging process of thermal energy storage system with a thermocline tank and pyrolysis setup.

different indexes were measured from experiment can calculated. These three indexes included energy efficiency, capacity ratio and utilization ratio. When the system is in charging mode its efficiency can be found as the ratio between the energy storage in heat transfer fluid (HTF) and the input energy which included energy transferred from the heating source (E_{HS}) and energy required by the pump $E_{inlet,pump}$) at steady state. On the other hand, the efficiency during discharge cycle can be calculated as the ratio between energy output from the outlet of thermocline tank and the energy required for pump work as shown in equation. Finally, the overall efficiency can be calculated as the ratio between output energy and total input energy included energy from heating source and total pump energy required for both charge/discharge mode in Eq. (1).

$$\eta_{C+} = \frac{E_{HTF}}{E_{inlet,pump} + E_{HS}} \tag{1}$$

where η_{C+} is charging efficiency, E_{HTF} is energy stored in molten salt system or the heat transfer fluid, and E_{HS} is the energy input from heating source.

Efficiency of energy storage during the discharging period can be found as a ratio between output energy after discharge and the total energy input for discharge period which is the combination of energy consumed by discharge pump and energy storage in heat transfer fluid during discharge period in Eq. (2).

$$\eta_{D-} = \frac{E_{output}}{E_{outlet,pump} + E_{HTF}} \tag{2}$$

where η_{D-} is the efficiency of the discharging mode, E_{output} is energy released from the thermocline tank for utilization, and $E_{outlet,pump}$ is the energy required to pump heat transfer fluid out of the thermocline tank using Eqs. (3) and (4).

$$E_{HTF} = E_{HTF,A} - E_{HTF,B} \tag{3}$$

where $E_{HtF,A}$ is energy that is transferred from molten salt to filler after charging the thermocline tank and $E_{HTF,B}$ is energy that is transfer from molten salt to filler before charging the thermocline tank.

$$E_{pump} = \int_{t_{start}}^{t_{end}} \frac{m}{\rho_{HTF}} \Delta P \ dt \tag{4}$$

where t_{start} , represent the initial state of charge, t_{end} represent the time it took to complete charge the thermocline tank, \dot{m} is the flowrate of molten salt, ρ_{HTF} is density of the molten salts system which included graphene oxide, nitrate based molten salt, and SiO₂.

The overall efficiency included both charge and discharge action under similar operating conditions. The equation for overall efficiency can be found by Eq. (5).

$$\eta_{\text{overall}} = \frac{E_{\text{outlet}}}{E_{\text{input}} + E_{\text{inlet,pump}} + E_{\text{ontlet,pump}}}$$
(5)

where $\eta_{overall}$ is overall efficiency of the thermocline system, E_{outlet} is energy monitored at the heat exchanger after it flow passed the thermocline tank, E_{input+} is energy released from the heating source, Einlet, pump/Eoutlet, pump is how much energy required to overcome friction in the tank and piping systems.

Capacity ratio is the ratio between total energy stored in the thermocline tank to the maximum possible storage energy during the charging cycle, which is shown in Eq. (6).

$$\alpha = \frac{E_{HTF}}{E_{Max}} \tag{6}$$

where α is capacity ratio, E_{HTF} is energy stored in the heat transfer fluid, and E_{Max} is the maximum energy storage derived from theoretical calculations.

Utilization ratio is the ratio between actual energy released to the maximum possible energy stored during the charging mode using Eq. (7).

Research article Engineered Science

$$\beta = \frac{E_{output}}{E_{Max}} \tag{7}$$

Energy released during the discharge mode (E_{output}) can be found as the difference between stored energy measured after charging the thermocline tank and stored energy measured after the complete discharge of thermocline tank. The theoretical maximum or peak energy can be calculated by Eq. (8).

$$E_{Max} = m_{HTF} \left[c_{p,solid} \left(T_{ss} - T_{HTF,i} \right) + \Delta h_f + C_{p,liquid} \left(T_{input} - T_{Sl} \right) \right]$$
(8)

where m_{HTF} is the mass of heat transfer fluid used during experiment, $c_{p,solid}$ is the specific heat capacity of solids in the thermocline tank (molten salts, graphene oxide and SiO₂), $C_{p,liquid}$ is the specific heat capacity of liquid molten salts.

2.4 Characterization of molten salt system

Encapsulated molten salt is a novel material composite with very few characterizations information. A scanning electron microscopy was used to capture morphology images of the encapsulated samples. It is important to investigate the presence of graphene oxide on the encapsulated matrix to guarantee the desirable structure. Additionally, X-ray diffraction (XRD) patterns were collected to compare chemical composition of molten salts before and after encapsulation. Diffraction patterns of graphene oxide and SiO₂ were also analyzed to observe how they impact chemical composition. Thermal capacities of the encapsulated molten salts compared to conventional molten salts (nitrate-based molten salts) was analyzed with a differential scanning calorimeter. The operation conditions begin at room temperature, ramped temperature to 140 °C at 15°C/min and then increased temperature to 300 °C at 10 °C/min under nitrogen flow. Area under the analytical curves from DSC measurements are then integrated to calculate heat loss or gain during both the exothermic and endothermic heat transfer process. Melting (T_m) and crystallization (T_c) temperature were also spotted as the peaks of DSC curves during both

exothermic (T_c) and endothermic process (T_m).

2.5 Pyrolysis reactor and setup

The production process of high-octane fuel started by adding 50 kilograms of cleaned and dried plastic bags in the reactors (add 25 kilograms to Reactor I and another 25 kilograms to Reactor II) as shown in Fig. 2. Different ratios of catalyst-towaste plastic were loaded into Hot Filter. After the plastic waste and catalyst are loaded, both low and high temperature condensing units are turned on and temperature monitored regularly. Flow of molten salt from thermal storage system were delivered into the spiral coil which flows into hot filter to reach a setpoint of 500 °C. The electrostatic precipitator (ESP) was turned on after temperature reached the setup. The temperature of reactor I and reactor II was then controlled by molten salt to reach setpoint. The pyrolysis reaction was then conducted for 15 minutes under stable operating conditions. The control system of pyrolysis consisted of programmable logic controller (PLC) to control flowrate of molten salt into the reactors and hot filter which allow temperature to be controlled. Three catalysts, namely ZSM-5, dolomite, and kaolin clay were studied. Other operating parameter included ratio of catalyst-to-plastic (0.1 - 0.3) and pyrolysis temperature $(300 - 500 \, ^{\circ}\text{C})$.

3 Results and discussion

3.1 Characterization of molten salt system

The Morphology of graphene oxide in molten salt matrix used as heat transfer agent during charge and discharge cycle was examined using SEM. The encapsulated graphene oxide pellet as shown in Fig. 3a (magnification of 1000) displayed tetrahedral like structure which demonstrated high oxidation during the preparation of graphene oxide via chemical process. Further magnification of the encapsulated surface revealed proper insertion of graphene oxide particles in SiO₂ composite Fig. 3b. Additionally, higher magnification confirmed the presence of nanoparticles, which successfully adhered to the composite's surface contributing to higher heat transfer capability.

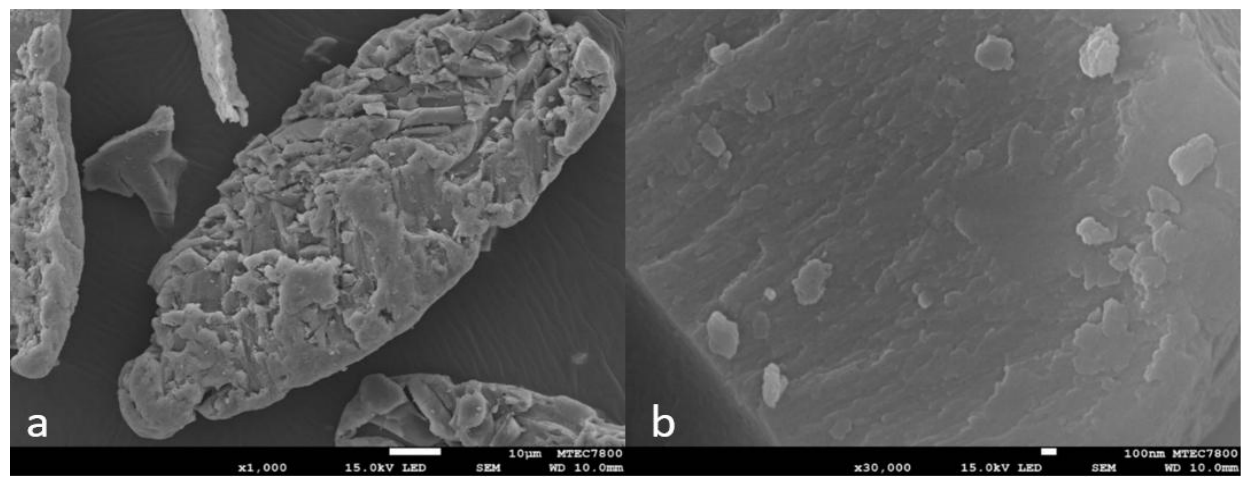
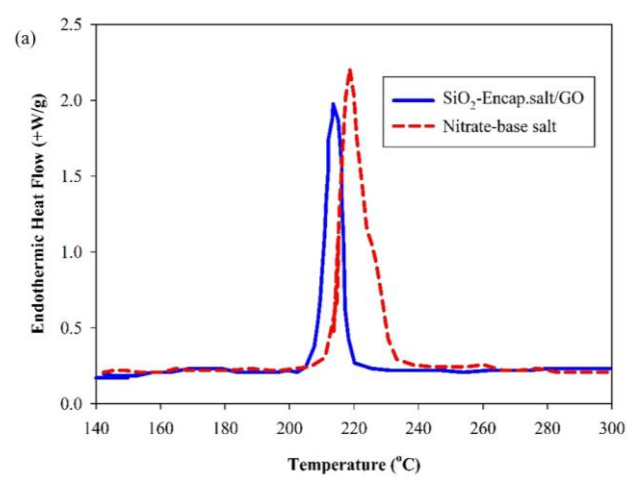


Fig. 3: SEM image magnification a) x1,000 and b) x30,000 (zoomed in red box from a) of encapsulated molten salt in graphene oxide matrix.



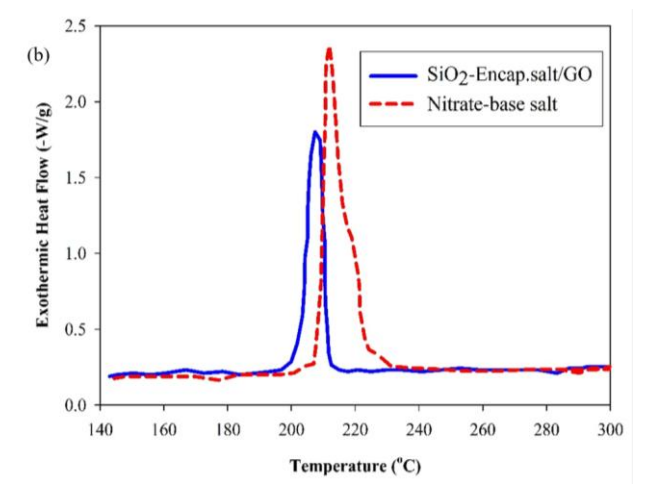


Fig. 4: Exothermic Heat flow representing crystallization temperature of plain nitrate-base salt and nitrate-base salt encapsulated in SiO₂/graphene oxide for a) endothermic and b) exothermic analysis.

Release of excess heat and energy storage ability of the triple molten salts system was investigated through DSC technique, as illustrated in Fig. 4. The peak location of DSC exothermic curves identified as the solidification step. DSC graph demonstrated the latent heat during phase change (area under the curve), melting temperature of the molten salt solution (peak temperature of the endothermic curve), and the onset temperature which indicated the temperature at which sample started to undergo phase change. Fig. 4a compared DSC endothermic curve from nitrate-based salt (40% KNO₃/60% NaNO₃ system) with the novel encapsulated system. Encapsulation of molten salt with graphene oxide caused the DSC exothermic curve to shift to the left indicating lower glass transition and melting temperature compared with conventional nitrate-based salts. The glass transition temperature and melting temperature of encapsulated molten salts were approximately 194 °C and 210 °C. On the other hand, glass transition and metaling temperature of conventional molten salt were roughly 211 °C and 224 °C. Fig. 4b demonstrated the DSC exothermic curve of both molten salt systems. Encapsulation of molten salt in graphene oxide and SiO₂ matrix resulted in a reduction in crystallization temperature from 219 °C to 203 °C.

XRD patterns of nitrated-based and encapsulated molten salts in Fig. 5 demonstrated three different oxide phases including NaNO₃, KNO₃ and LiNO₃. Presence of molten salts inside the encapsulation demonstrate successful adhesion to SiO₂ structures. It was also observed that graphene oxide does not have a significant impact on the crystallinity of the encapsulated materials. This indicated that graphene oxide is successfully trapped inside SiO₃ matrix. Presence of crystalline NaNO₃ (represented as α) was detected at 2 θ of 27°, 35°, and 56°. Additionally, KNO₃ was detected as 18°, 20°, 32°, 38°, 41° and 44°. LiNO₃ was observed at 2 θ of 33°.

3.2 Charge and discharge performance testing

Fig. 6 demonstrates temperature distribution of molten salt system in axial direction at different locations from top of the

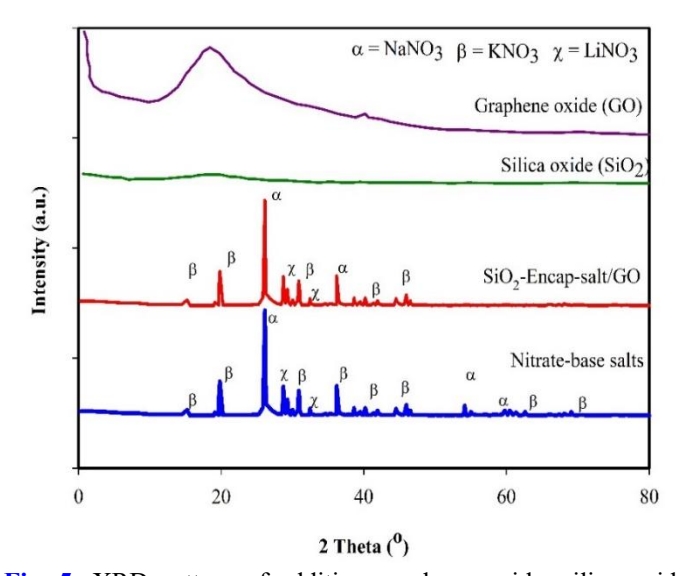


Fig. 5: XRD pattern of additive graphene oxide, silica oxide, encapsulated molten salt and plain nitrate-base salts.

thermocline tank to the bottom. It is observed that the molten salt system has a significant impact on thermal transfer performance inside the thermocline tank. Impact on heat transfer propagation inside the thermocline tank was investigated by varying molten salt flowrate, as shown in Fig. 6. Initial temperature inside the thermocline tank set at 150 °C in order to transform molten salt into an aqueous phase. A heating source was set at 300 °C to charge molten salt before it is delivered into the bottom of the thermocline tank. After charging for 34.5 minutes, it was observed that temperature gradient started to form 0.35 meter above the molten salt inlet channel. The temperature gradient moved up significantly after 60 minutes of charging, indicating an efficient heat transfer capability between encapsulated molten salt and spherical ceramic filters. Ceramic balls were used to create turbulence in flow of molten salt which will enhance heat transfer inside thermocline tanks. It also acts as a heat adsorber which provides a significant heat storage capacity during charge and discharge phase. After 111.8 minutes of Research article Engineered Science

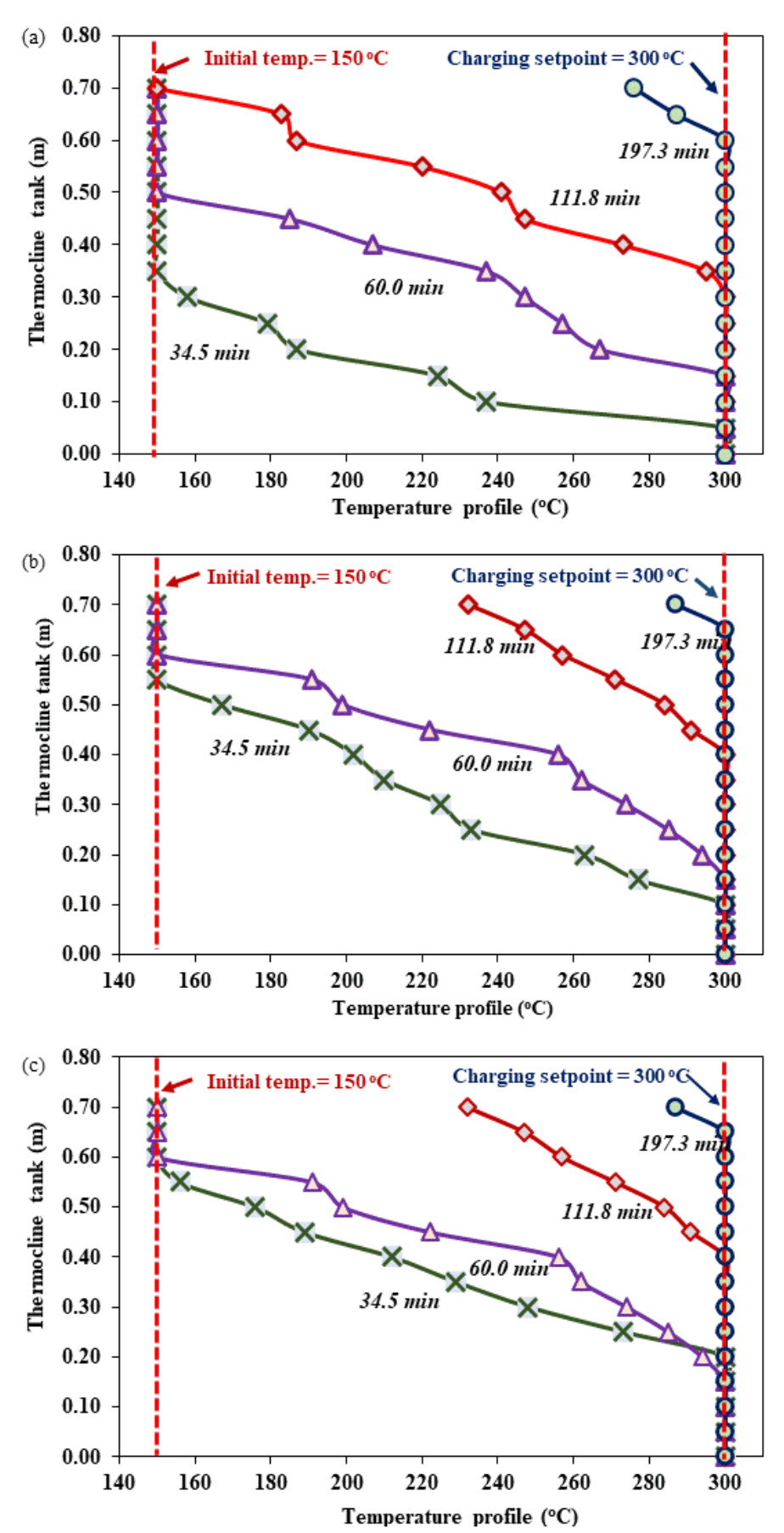


Fig. 6: Temperature profile of thermocline tank charging performed at (a) 0.3 m³/h, (b) 0.5 m³/h and (c) 0.7 m³/h flowrate of heat transfer fluid (encapsulated molten salt on graphene oxide).

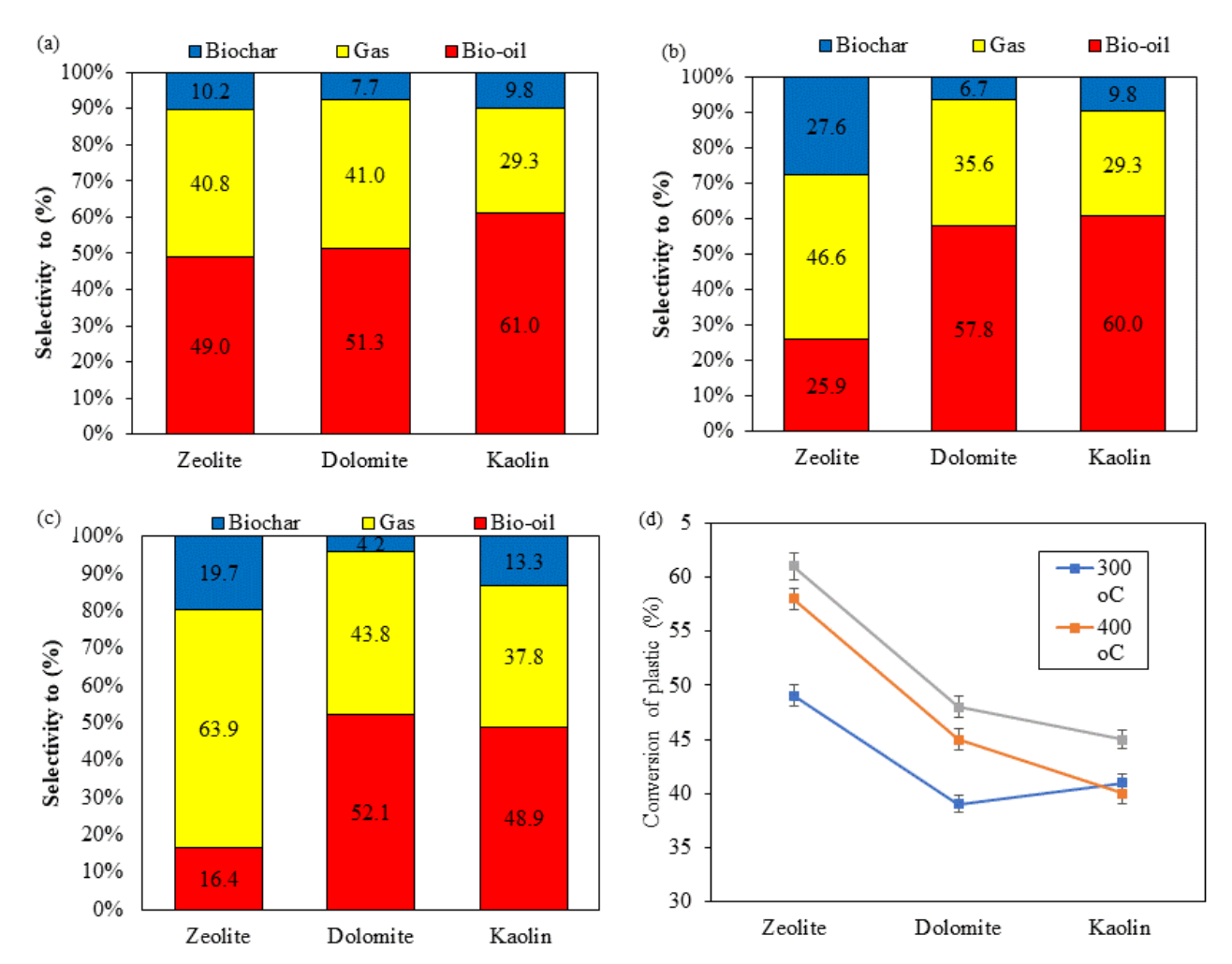


Fig. 7: Influence of pyrolysis temperature and type of catalyst on selectivity toward bio-oil, gas and biochar products: (a) 300 °C, (b) 400 °C, (c) 500 °C and (d) conversion of plastic waste.

charging approximately 50% of thermocline tank is successfully charged to 300 °C. A charging state of 90% is reached approximately after 197.3 minutes of operation. An increase in flow rate of molten salt was found to also improve the rate of heat transfer throughout the axial direction of the thermocline tank as shown in Figs. 6b and 6c. Data acquired correlated well with documented reports from other researches.[34] An increase in heat transfer efficiency is due to the formation of turbulent flow as intensified vortexed formed when molten salt collided with ceramic filer inside the thermocline tank.[35,36] From performance testing experiments it was also found that graphene oxide help improve heat transfer mechanisms. Many studies have shown presence of graphene oxide can increase Nusselt ratio which illustrated the ratio between convection and conduction heat transfer mode.[37]

3.3 Pyrolysis performance testing

Pyrolysis of waste plastic bag were conducted in two fixedbed reactors with double condensation trap producing shorter chain molecules in the form of bio-oil, biochar and gaseous products. Pyrolysis mechanism usually proceeds in two main

stages including primary pyrolysis and secondary cracking. An increase in temperature was found to improve formation of biooil from alkaline type catalyst such as dolomite and kaolin. A selectivity of 49% toward biooil was observed when pyrolysis temperature was set at 300 °C over zeolite catalyst as shown in Fig. 7a. However, as temperature increased the secondary cracking reaction started to take place causing volatile products to be breakdown in to gaseous products.[38] Additionally, zeolite catalysts contained acidic active sites causing attached molecules to exchange protons with acidic sites causing molecules to spit into smaller molecules.[39,40] For this reason, gaseous product from zeolite catalyst increased from 40.8% to 63.9%, while biooil decreased from 49.0%. Approximately 2.5 to 10.0% biochar was formed due to conversion of graphite product on heterogeneous catalyst to hard coke inside catalyst's pore. [41] An increase in temperature was also found to cause biochar content to increase as shown in Figs. 7b-c. This is because as the temperature increased more reactant was allowed to enter catalyst pore resulting in carbon accumulation. Formation of biochar was suppressed

Research article **Engineered Science**

when alkaline type catalysts (dolomite and kaolin) were used. Innovation (TSRI), Fundamental Fund, fiscal 2025. These results corresponded with other researches in the field of pyrolysis experiments. [42,43] The conversion of waste plastic was found to increase temperature rises as shown in Fig. 7d. For zeolite catalysts, conversion started at 48.1% at 300 °C, and increased to 61.3% as temperatures increased to 500 °C. Raschat et al. and Sun et al. also reported pyrolysis of plastic to yield 63% biooil.[44,45] Temperature was also found to have a significant impact on pyrolysis of waste cooking oil, which corresponds well with results from this research.[46] Almost 40% diesel was found in biooil product, however due to high acidic content the biooil have to be treated under high temperature and hydrogen pressure environment under palladium-base catalyst. An example of palladium-based catalyst with humic acid modified was successfully developed. which can be employed for the hydrotreating process of biooil.[47] Statistical analysis of data obtained reveals a standard error of 0.5 to 1.2%.

4. Conclusion

The objective of this research is to develop a solar thermalbased pyrolysis system to convert waste plastic bag to combustible biooil. Innovative encapsulated molten was system was investigated as heat transfer agent inside thermocline tank used to storage solar heat for the pyrolysis of waste plastic bag to biooil. Morphology analysis via, SEM and XRD method revealed that the integrity of the encapsulated is not affected by the impregnated graphene oxide which help facilitate enhancement of heat transfer inside the system. DSC analysis of liquid molten salt demonstrated 10% lower melting point temperature after graphene oxide was encapsulated in the system. Charging and discharging test of the thermocline system revealed an improvement in heat transfer efficiency as flowrate of molten salt system increased. Pyrolysis of waste plastic bag was conducted over different heterogeneous catalysts including zeolite, dolomite and kaolin. Gaseous products increased over zeolite catalyst as pyrolysis temperature increases due to the cracking reaction which cause volatile molecules to be broken down furthermore. Utilization of alkaline type catalysts, such as kaolin was capable of suppressing formation of gaseous product and biochar. The highest amount of biooil obtained was 61%, which was derived from kaolin catalyst at a pyrolysis temperature of 300 °C. Data obtained can be used to upscale production of biooil from waste plastic bag via pyrolysis reaction.

Acknowledgement

Conflict of Interest

There is no conflict of interest.

Supporting Information

Not applicable.

References

- [1] E. Dogan, M. Z. Chishti, N. Karimi Alavijeh, P. Tzeremes, The roles of technology and Kyoto Protocol in energy transition towards COP26 targets: Evidence from the novel GMM-PVAR approach for G-7 countries, Technological Forecasting and Social Change. 2022, 181. 121756, doi: 10.1016/j.techfore.2022.121756.
- [2] C. Tolliver, A. R. Keeley, S. Managi, Policy targets behind green bonds for renewable energy: Do climate commitments matter? Technological Forecasting and Social Change, 2020, 157, 120051, doi: 10.1016/j.techfore.2020.120051.
- [3] S. Ladkany, W. Culbreth, N. Loyd, Molten salts and applications II: 565 °C molten salt solar energy storage design, corrosion, and insulation, Journal of Energy and Power 2018, 12: 517-532, doi: 10.17265/1934-Engineering, 8975/2018.11.002.
- [4] A. Abdelfatah, A. M. Raslan, L. Z. Mohamed, Corrosion characteristics of 304 stainless steel in sodium chloride and sulfuric acid solutions, International Journal of Electrochemical Science, 2022, 17, 220417, doi: 10.20964/2022.04.29.
- [5] Q. Gao, Y. Lu, Y. Wang, Y. Wu, C. Zhang, Y. Wang, Electrochemical study on the corrosion behavior of 316L stainless steel in quaternary nitrate molten salt nanofluids for thermal energy storage applications, Journal of Energy Storage, 2024, **83**, 110491, doi: 10.1016/j.est.2024.110491.
- [6] M. Luqman, T. Al-Ansari, A novel integrated wastewater recovery, clean water production and air-conditioning system, Energy Conversion and Management, 2021, 244, 114525, doi: 10.1016/j.enconman.2021.114525.
- [7] J. Ma, Y. Li, X. Wei, Z. Li, G. Li, T. Liu, Y. Zhao, S. He, Y. Li, R. Li, C. Gu, J. Li, H. Lu, Q. Wang, K. Li, C. Liu, Molten saltassisted encapsulation of prussian blue with carbon for highperformance potassium-ion storage, Chemical Engineering *Journal*, 2022, **433**, 133777, doi:10.1016/j.cej.2021.133777.
- [8] Y. Hou, J. Qiu, W. Wang, X. He, M. Ayyub, Y. Shuai, Development of topology-optimized structural cavities macroencapsulating chloride salt by gel-casting for high-temperature thermal energy storage, Journal of Energy Storage, 2024, 78, 110056, doi: 10.1016/j.est.2023.110056.
- [9] J. F. Hoffmann, T. Fasquelle, V. Goetz, X. Py, A thermocline This research is supported by Thailand Science Research and thermal energy storage system with filler materials for

concentrated solar power plants: Experimental data and numerical model sensitivity to different experimental tank scales, Applied Thermal Engineering, 2016, 100, 753-761, doi: 10.1016/j.applthermaleng.2016.01.110.

- [10] N. Saardchom, Bioeconomy as a new S-curve for Thai economy, Agricultural Economics - Czech, 2017, 63, 430-439, doi: 10.17221/78/2016-AGRICECON.
- [11] S. Vannerem, P. Neveu, O. Falcoz, Experimental and numerical investigation of the impact of operating conditions on thermocline storage performance, Renewable Energy, 2021, 168, 234-246, doi: 10.1016/j.renene.2020.12.061.
- [12] M. Cascetta, M. Petrollese, J. Oyekale, G. Cau, Thermocline vs. two-tank direct thermal storage system for concentrating solar power plants: a comparative techno-economic assessment, International Journal of Energy Research, 2021, 45, 17721-17737, doi: 10.1002/er.7005.
- [13] S. Oian, J. F. L. Duval, Y. B. Gianchandani, O. Tabata, H. Zappe, Mixers, Comprehensive Microsystems, 2016, 2, 323-373, [24] S. M. Al-Salem, S. R. Chandrasekaran, A. Dutta, B. K. doi: 10.1016/B978-044452190-3.00043-4.
- [14] Y. Zhang, J. Wu, W. Wang, J. Ding, J. Lu, Experimental and numerical studies on molten salt migration in porous system with phase change, International Journal of Heat and Mass Transfer, 2019. 129. 397-405, 10.1016/j.ijheatmasstransfer.2018.09.122.
- [15] A. Bruch, J. F. Fourmigué, R. Couturier, Experimental and numerical investigation of a pilot-scale thermal oil packed bed thermal storage system for CSP power plant, Solar Energy, 2014, liquid oil from the pyrolysis of waste high-density polyethylene 105, 116-125, doi: 10.1016/j.solener.2014.03.019.
- [16] K. J. Brewster, J. R. Fosheim, W. J. Arthur-Arhin, K. E. Schubert, M. Chen-Glasser, J. E. Billman, G. S. Jackson, Particlewall heat transfer in narrow-channel bubbling fluidized beds for thermal energy storage, International Journal of Heat and Mass Transfer, 2024. 224. 125276, 10.1016/j.ijheatmasstransfer.2024.125276.
- [17] G. Jia, X. Yuan, Y. Cao, Y. Yun Cao, K. Jiang, K. Ke Jiang, Y. Yang, Z. Chen, Z. Chen, G. Cheng, Z. Yang, Y. Zou, Experimental and numerical investigation into a thermocline storage for district heating, *Applied Thermal Engineering*, 2024, 245, 122748, doi: 10.1016/j.applthermaleng.2024.122748.
- [18] M. W. K. Jaber, A. Güngör, E. Canli, A. H. Abdulkarim, U. Sentürk, Transient evolution of thermal stratification and passive flow guidance inside a heat exchanger immersed thermal energy storage tank, Journal of Energy Storage, 2024, 88, 111472, doi: 10.1016/j.est.2024.111472.
- [19] N. Promsampao, N. Chollacoop, A. Pattiya, Bio-oil Fuels, 2018, 2, 1057-1068, doi: 10.1039/c8se00040a. production from palm kernel cake using fast-pyrolysis process, Engineered Science, 2024, 31, 1179, doi: 10.30919/es1179.
- Hemathulin, C. Turakarn, K. Chaiphet, P. Rattanadecho, Addition 2024, 10, e26702, doi: 10.1016/j.heliyon.2024.e26702.

of hydrocarbon components to products in the catalytic pyrolysis of sawdust by natural catalysts, Engineered Science, 2004, 31, 1194. doi: 10.30919/es1194.

- [21] C. AlGemayel, J. Zeaiter, S. Talih, N. A. Saliba, A. Shihadeh, Mechanistic analysis of the pyrolysis of vegetable glycerin: a reactive force field - molecular dynamics study, Engineered Science, 2023, 23, 885. doi: 10.30919/es885.
- [22] M. M. Hasan, R. Haque, M. I. Jahirul, M. G. Rasul, Pyrolysis of plastic waste for sustainable energy Recovery: Technological advancements and environmental impacts, Energy Conversion and 326. 119511. Management, 2025. doi: 10.1016/j.enconman.2025.119511.
- [23] B. L. F. Chin, S. Yusup, A. Al Shoaibi, P. Kannan, C. Srinivasakannan, S. A. Sulaiman, Kinetic studies of co-pyrolysis of rubber seed shell with high density polyethylene, *Energy* Conversion and Management, 2014, 87, 746-753, doi: 10.1016/j.enconman.2014.07.043.
- Sharma, Fuel. 2021, 304, 121396, doi: 10.1016/i.fuel.2021.121396.
- [25] M. M. Hasan, M. G. Rasul, M. I. Jahirul, M. M. K. Khan, Characterization of pyrolysis oil produced from organic and plastic wastes using an auger reactor, Energy Conversion and Management, 2023, 278, 116723, doi: 10.1016/j.enconman.2023.116723.
- [26] F. A. Aisien, E. T. Aisien, Production and characterization of plastics using spent fluid catalytic cracking catalyst, Sustainable Chemistry for Climate Action, 2023, 2, 100020, doi: 10.1016/j.scca.2023.100020.
- [27] Y. Misra, D. J. Prasanna Kumar, R. K. Mishra, V. Kumar, N. Dwivedi, Thermocatalytic pyrolysis of plastic waste into doi: renewable fuel and value-added chemicals: a review of plastic types, operating parameters and upgradation of pyrolysis oil, Water-Energy Nexus, 2025. 55-72. doi: 10.1016/j.wen.2025.03.002.
 - [28] K. M. Rajendran, V. Chintala, A. Sharma, S. Pal, J. K. Pandey, P. Ghodke, Review of catalyst materials in achieving the liquid hydrocarbon fuels from municipal mixed plastic waste (MMPW), Materials Today Communications, 2020, 24, 100982, doi: 10.1016/j.mtcomm.2020.100982
 - [29] M. V. Singh, S. Kumar, M. Sarker, Waste HD-PE plastic, deformation into liquid hydrocarbon fuel using pyrolysiscatalytic cracking with a CuCO₃ catalyst, Sustainable Energy &
- [30] N. H. Dassi Djoukouo, B. M. K. Djousse, H. G. Doukeng, D. A. M. Egbe, J. K. Tangka, M. Tchoffo, Design of a pyrolyser [20] N. Pannucharoenwong, S. Echaroj, K. Duanguppama, S. model for the conversion of thermoplastics into fuels, *Heliyon*,

Research article **Engineered Science**

- Advances in plastic to fuel conversion: reactor design, operational optimization, and machine learning integration, Sustainable Energy & Fuels, 2024, 9. 54-71, doi: 10.1039/d4se01045k.
- [32] B. Luo, Z. Tian, C. Wang, Y. Chen, J. Liu, R. Shu, Highly stable Co@BC catalysts encapsulated in biochar for efficient lignin hydrogenolysis to valuable monophenols, *Industrial Crops* and Products. 2024. 222. 120076. 10.1016/j.indcrop.2024.120076.
- [33] A. Rafiani, D. Aulia, G. T. M. Kadja, Zeolite-encapsulated catalyst for the biomass conversion: Recent and upcoming advancements, Case Studies in Chemical and Environmental Engineering, 2024, 9, 100717, doi: 10.1016/j.cscee.2024.100717. [34] M. Cheng, J. Yang, H. Chi, H. Yao, Influence characteristic and improvement mechanism of thermal storage performance of Packed-bed thermocline tank based on high-temperature molten salt, Journal of Energy Storage, 2024, 101, 113976, doi: 10.1016/j.est.2024.113976.
- [35] D. Nualsing, N. Pannucharoenwong, S. Echaroj, K. Duanguppama, P. Rattanadecho, Investigation of nanofluid molten salts in a thermocline tank as a thermal energy storage system, Asia-Pacific Journal of Science and Technology, 2024, 29, 1-7, doi: 10.14456/apst.2024.69.
- [36] D. Nualsing, N. Pannucharoenwong, S. Echaroj, P. Rattanadecho, Investigation of molten salts incorporated with transfer efficiency, Case Studies in Thermal Engineering, 2023, 49, 103258, doi: 10.1016/j.csite.2023.103258.
- [37] P. Kumar, B. Yadav, A. Kumar, C. Bora, A. Kumar, S. Das, An experimental study on heat transfer performance of GO and rGO-CuO nanofluids in a heat exchanger, *FlatChem*, 2021, 27, 100245, doi:10.1016/j.flatc.2021.100245.
- [38] M. S. Hammed, F. Sayed, Reply to the discussion of Moustafa (2021) on sayed et al. (2020) (marine and petroleum geology, 17, 2020-104401), Marine and Petroleum Geology, 2022, **143**, 105789, doi: 10.1016/j.marpetgeo.2022.105789.
- [39] S. Echaroj, M. Santikunaporn, A. N. Phan, Supercritical ethanol liquefaction of bamboo leaves using functionalized reduced graphene oxides for high quality bio-oil production, Renewable Energy, 2023, 204. 848-857, doi: 10.1016/j.renene.2022.12.110.
- [40] N. Pannucharoenwong, K. Duanguppama, S. Echaroj, C. Turakarn, K. Chaiphet, P. Rattanadecho, Improving fuel quality from plastic bag waste pyrolysis by controlling condensation temperature, *Energy Reports*, 2023, 9, 125-138, doi: 10.1016/j.egyr.2023.05.231.
- Biochar modification to enhance sorption of inorganics from exceeds the permitted use, you will need to obtain permission

[31] K. Paavani, K. Agarwal, S. S. Alam, S. Dinda, I. Abrar, water, Bioresource Technology, 2017, 246, 34-47, doi: 10.1016/j.biortech.2017.07.082.

- [42] H. Sui, Y. Chen, H. Chen, Y. Zhao, C. Tian, W. Chen, C. Chang, S. Pang, P. Li, Characterization and mechanistic insights into coke formation on biochar-based catalysts under microwaveassisted biomass pyrolysis, *Industrial Crops and Products*, 2025, 226, 120645, doi: 10.1016/j.indcrop.2025.120645.
- [43] J. Li, K. Xu, X. Yao, J. Liu, D. S. Su, B. Wang, Study on the doi: effect of biochar catalyst on the formation of biomass slow Fuel. 2025. 392. 134862. pyrolysis products, doi:10.1016/j.fuel.2025.134862.
 - [44] P. Moonsin, W. Roschat, S. Phewphong, S. Watthanalao, P. Chaona, B. Maneerat, S. Arthan, A. Thammayod, T. Leelatam, K. Duanguppama, B. Yoosuk, P. Janetaisong, V. Promarak, The physicochemical characterization of diesel-like fuels derived from plastic waste pyrolysis, Journal of the Taiwan Institute of Chemical Engineers. 2025, 171, 106040, 10.1016/j.jtice.2025.106040.
 - [45] D. Sun, L. Sun, D. Han, L. Chen, S. Yang, T. Li, Z. Dong, B. Zhao, M. Xu, S. Tian, X. Xie, H. Si, D. Hua, Enhanced aromatics production via co-pyrolysis of biomass and plastic by Zn modified ZSM-5 catalysts, Journal of Analytical and Applied *Pyrolysis*, 2025, **189**, 107086, doi: 10.1016/j.jaap.2025.107086.
 - [46] W. Banchapattanasakda, C. Asavatesanupap, Santikunaporn, *Engineered Science*, 2024, **31**, 1211, doi: 10.30919/es1211.
- anodic aluminum oxide as thermal energy storage fluid on heat [47] I. M. Dzheldybaeva, Z. K. Kairbekov, M. Z. Esenalieva, A. Z. Kairbekov, S. M. Suimbaeva, D. Z. Abil'mazhinova, Humic acid modified applied palladium catalysts for nitro compounds reduction, Engineered Science, 2023, 26, 1001, doi: 10.30919/es1001.

Publisher's Note: Engineered Science Publisher remains neutral with regard to jurisdictional claims in published maps and institutional affiliations.

Open Access

This article is licensed under a Creative Commons Attribution 4.0 International License, which permits the use, sharing, adaptation, distribution and reproduction in any medium or format, as long as appropriate credit to the original author(s) and the source is given by providing a link to the Creative Commons license and changes need to be indicated if there are any. The images or other third-party material in this article are included in the article's Creative Commons license, unless indicated otherwise in a credit line to the material. If material is not included in the article's Creative Commons license and [41] T. Sizmur, T. Fresno, G. Akgül, H. Frost, E. Moreno-Jiménez, your intended use is not permitted by statutory regulation or

directly from the copyright holder. To view a copy of this license, visit http://creativecommons.org/ licenses/by/4.0/.

©The Author(s) 2025